The Journal of Immunology

Requirement for MyD88 Signaling in B Cells and Dendritic Cells for Germinal Center Anti-Nuclear Antibody Production in Lyn-Deficient Mice

Zhaolin Hua, Andrew J. Gross, Chrystelle Lamagna, Natalia Ramos-Hernández, Patrizia Scapini, Ming Ji, Haitao Shao, Clifford A. Lowell, Baidong Hou and Anthony L. DeFranco

J Immunol 2014; 192:875-885; Prepublished online 30 December 2013;
doi: 10.4049/jimmunol.1300683
http://www.jimmunol.org/content/192/3/875

The Journal of Immunology is published twice each month by
The American Association of Immunologists, Inc.,
1451 Rockville Pike, Suite 650, Rockville, MD 20852

Print ISSN: 0022-1767 Online ISSN: 1550-6606.

Requirement for MyD88 Signaling in B Cells and Dendritic Cells for Germinal Center Anti-Nuclear Antibody Production in Lyn-Deficient Mice

Zhaolin Hua,* Andrew J. Gross,†,‡ Chrystelle Lamagna,§ Natalia Ramos-Hernández,† Patrizia Scapini,§,¶ Ming Ji,† Haitao Shao,* Clifford A. Lowell,§ Baidong Hou,*,† and Anthony L. DeFranco†

The intracellular tyrosine kinase Lyn mediates inhibitory receptor function in B cells and myeloid cells, and *Lyn*$^{-/-}$ mice spontaneously develop an autoimmune and inflammatory disease that closely resembles human systemic lupus erythematosus. TLR-signaling pathways have been implicated in the production of anti-nuclear Abs in systemic lupus erythematosus and mouse models of it. We used a conditional allele of *Myd88* to determine whether the autoimmunity of *Lyn*$^{-/-}$ mice is dependent on TLR/MyD88 signaling in B cells and/or in dendritic cells (DCs). The production of IgG anti-nuclear Abs, as well as the deposition of these Abs in the glomeruli of the kidneys, leading to glomerulonephritis in *Lyn*$^{-/-}$ mice, were completely abolished by selective deletion of *Myd88* in B cells, and autoantibody production and glomerulonephritis were delayed or decreased by deletion of *Myd88* in DCs. The reduced autoantibody production in mice lacking MyD88 in B cells or DCs was accompanied by a dramatic decrease in the spontaneous germinal center (GC) response, suggesting that autoantibodies in *Lyn*$^{-/-}$ mice may depend on GC responses. Consistent with this view, IgG anti-nuclear Abs were absent if T cells were deleted (TCRβ$^{-/-}$ TCRδ$^{-/-}$ mice) or if T cells were unable to contribute to GC responses as the result of mutation of the adaptor molecule SAP. Thus, the autoimmunity of *Lyn*$^{-/-}$ mice was dependent on T cells and on TLR/MyD88 signaling in B cells and in DCs, supporting a model in which DC hyperactivity combines with defects in tolerance in B cells to lead to a T cell–dependent systemic autoimmunity in *Lyn*$^{-/-}$ mice. ***The Journal of Immunology*, 2014, 192: 875–885.**

The human autoimmune disease systemic lupus erythematosus (SLE) is characterized by production of autoantibodies against multiple self-Ags, of which nuclear autoantigens, such as dsDNA and ribonucleoproteins (RNPs), are predominant (1). A similar spontaneously developing autoimmunity characterized by anti-nuclear Ab production is seen in a variety of genetically determined mouse models, some of which are multigenic and others of which result from spontaneous or targeted mutations of known genes (2). One of the better studied of the latter category is the *Lyn*$^{-/-}$ mouse, which develops a highly penetrant autoimmune and inflammatory disease characterized by anti-dsDNA IgG Abs and glomerulonephritis (3–5). Lyn is a Src family protein tyrosine kinase that is required for the function of a number of inhibitory receptors on B cells and myeloid cells. In B cells, the functions of both the sialic acid–binding Ig superfamily member CD22 and of the inhibitory FcγRIIB depend on the ability of Lyn to phosphorylate tyrosines in their cytoplasmic tails, catalyzing the recruitment to the membrane of the inhibitory phosphatases SHP-1 and SHIP-1 (4, 6, 7). Autoimmunity of Lyn-deficient mice likely involves a combination of compromised tolerance of B cells, which is due to the loss of these inhibitory pathways, and hyperactivity of myeloid cells, which drive activation of T cells and inflammatory disease (8–11).

Like most human autoimmune diseases, lupus has a strong genetic susceptibility component that is multigenic in the great majority of patients (1, 12). Among the genes that contribute to lupus susceptibility in humans are those encoding components of Lyn-inhibitory pathways. For example, some individuals of European descent have a single nucleotide polymorphism in the 5′ untranslated region of the *LYN* gene that is mildly protective for the development of lupus (odds ratio, 0.80) (12). More impressively, loss-of-function alleles of SIAE, which encodes a sialic acid acetyl esterase that is necessary to create the ligand for CD22, contributes a large increase in the susceptibility to lupus and several other autoimmune diseases (odds ratio, ~8) in a small, but significant, fraction of individuals (13). Given that *Lyn*$^{+/-}$ mice exhibit a mild lupus phenotype (14), it is possible that less frequent alleles of Lyn, other than those examined in genome-wide association analysis, and/or alleles of genes

*Key Laboratory of Infection and Immunity, Institute of Biophysics, Chinese Academy of Sciences, Beijing 100101, China; †Department of Microbiology and Immunology, University of California, San Francisco, San Francisco, CA 94143; ‡Department of Medicine, University of California, San Francisco, San Francisco, CA 94143; §Department of Laboratory Medicine, University of California, San Francisco, San Francisco, CA 94143; and ¶Division of Pathology, Department of Pathology and Diagnostics, University of Verona, Verona 37134, Italy

Received for publication March 12, 2013. Accepted for publication November 18, 2013.

This work was supported by research grants from the National Institutes of Health (R01AI072058 and P01AI078869 to A.L.D. and P01AI078869 and R01AI068150 to C.A.L.), as well as by the National Natural Science Foundation of China (Grants 31170848 to B.H. and 31200669 to Z.H.). B.H. is supported by an award from the National Thousand Talent Plan of China (2011).

Address correspondence and reprint requests to Dr. Anthony L. DeFranco or Dr. Baidong Hou, Department of Microbiology and Immunology, University of California, San Francisco, 513 Parnassus Avenue, Box 0414, HSE-1001F, San Francisco, CA 94143 (A.L.D.) or Key Laboratory of Infection and Immunity, Institute of Biophysics, Chinese Academy of Sciences, 15 Datun Road, Chaoyang District, Beijing 100101, China (B.H.). E-mail addresses: anthony.defranco@ucsf.edu (A.L.D.) or baidong_hou@sun5.ibp.ac.cn (B.H.)

The online version of this article contains supplemental material.

Abbreviations used in this article: ANA, anti-nuclear Ab; C3, complement 3; DC, dendritic cell; GC, germinal center; RNP, ribonucleoprotein; SLE, systemic lupus erythematosus; SmRNP, Smith Ag ribonucleoprotein; Tfh, follicular helper T.

www.jimmunol.org/cgi/doi/10.4049/jimmunol.1300683

encoding the other components of Lyn-dependent inhibitory pathways contribute significantly to lupus susceptibility in humans.

Recent studies (15) in several mouse models of lupus implicated TLR9 and TLR7 in the spontaneous production of anti-dsDNA and anti-RNP IgG, respectively. For example, MRL/lpr mice are protected from the development of glomerulonephritis when combined with loss-of-function mutation of TLR7, either alone or in combination with mutation of TLR9 (16). Similarly, deletion of the TLR-signaling component MyD88 prevents spontaneous lupus-like disease in Lyn-deficient mice (17). Conversely, the *Yaa* autoimmune accelerator locus of mice turns out to be a duplication onto the Y chromosome of a small region of the X chromosome that includes TLR7, resulting in increased expression of TLR7 (18–20). The possible relevance of TLR7 and TLR9 to lupus-like autoimmunity was initially suggested by in vitro studies of Marshak-Rothstein and coworkers (15), demonstrating a marked synergy for B cell activation in vitro between BCR engagement and TLR9 or TLR7 engagement. This synergy was shown to operate in vivo as well (21). Although those studies strongly suggest that the contribution of TLR7 and TLR9 to lupus-like autoantibody production is by their action in nucleic acid–recognizing B cells, TLR7 and TLR9 are also potent activators of dendritic cells (DCs) and, moreover, induce type 1 IFN production by plasmacytoid DCs (22). A number of studies implicated type 1 IFNs in the pathogenesis of human lupus (23), so it is also possible that the nucleic acid–recognizing TLRs play key roles in DCs for the development or propagation of lupus-like autoimmunity.

Recently, we used cell type–specific deletion of the key TLR-signaling component MyD88 to dissect the cellular basis for TLR9 stimulation of Ab responses to immunization. We found that in vivo IgG responses to soluble protein–CpG oligonucleotide conjugates were dependent primarily on TLR9/MyD88 signaling in DCs, whereas IgG responses to virus-like particles or inactivated influenza virus particles were primarily dependent on TLR/MyD88 signaling in B cells (24). In this study, we addressed the role of MyD88 signaling in B cells and in DCs for the spontaneous development of lupus-like autoimmunity in *Lyn*$^{-/-}$ mice. We found that anti-dsDNA and anti-RNP IgG in this model were likely produced by germinal center (GC) responses that were highly dependent on TLR/MyD88 signaling in B cells. TLR/MyD88 signaling in DCs also played a major, although less essential, role in autoantibody production. In contrast, TLR/MyD88 signaling in DCs was essential for accumulation of activated T cells and splenomegaly, reinforcing the notion that Lyn-deficient autoimmune disease has both autoantibody and inflammatory components and that TLR/MyD88 signaling contributes to both disease manifestations.

Materials and Methods

Mice

B6 (000664; C57BL/6J) mice were from The Jackson Laboratory. *Lyn*$^{-/-}$ *Myd88*^{fl} mice (B6.129P2-*Myd88*^{tm1Defr}), *Myd88*$^{fl/fl}$ *Cd11c-Cre* mice, and *Myd88*$^{fl/fl}$ *Cd79a-Cre* mice were described previously (25–27) and were backcrossed onto the C57BL/6 background for ≥10 generations. These mice were bred to generate *Lyn*$^{-/-}$ *Myd88*$^{fl/fl}$, *Lyn*$^{-/-}$ *Myd88*$^{fl/fl}$ *Cd79a-Cre*, or *Lyn*$^{-/-}$ *Myd88*$^{fl/fl}$ *Cd11c-Cre* mice used in this study. Sex-matched littermates were used in all experiments, and data were pooled and analyzed according to the age group. *Sap*$^{-/-}$ mice (28) were obtained from Dr. Pamela Schwartzberg (National Institutes of Health, Bethesda, MD). *tcrβ*$^{-/-}$ *tcrδ*$^{-/-}$ mice (29, 30) were from The Jackson Laboratory. Animals were housed in specific pathogen–free animal facilities at the University of California, San Francisco or the Institute of Biophysics under conditions that met the respective institutional and national guidelines. Animal use in each facility was approved by the respective Institutional Animal Care and Use Committee.

Anti-nuclear Ab immunofluorescence

Serum was diluted at 1:40 or 1:160 in PBS containing 1% FBS and applied to fixed and permeabilized HEp-2 anti-nuclear Ab (ANA) slides (Bio-Rad). After overnight incubation at 4˚C, ANAs were detected by Alexa Fluor 488–conjugated goat anti-mouse IgG (Fcγ fragment specific; Jackson ImmunoResearch). DAPI was included in the last wash of slides. Slides were visualized with a regular fluorescence microscope under a 40× objective lens and imaged with an Olympus digital camera. Nuclear regions were defined with DAPI staining, and the average Alexa 488 fluorescence intensity of nuclear regions was quantified with ImageJ (National Institutes of Health).

Serum Ig and autoantibody measurement

Levels of serum IgM and IgG were measured using ELISA-based quantification kits (Bethyl Laboratories), according to the manufacturer's instructions. For anti-dsDNA Ig ELISA, 96-well flat-bottom plates (BD Falcon) were coated with 20 ng/well linearized pUC19 plasmid in 100 mM Tris-HCl (pH 7.3). For anti-Smith Ag ribonucleoprotein (SmRNP) Ig ELISA, plates were coated with 2 U/ml Smith Ag RNP complex Ag (ImmunoVision) in carbonate buffer (pH 9.6). After overnight incubation at 4˚C, plates were blocked with PBS containing 1% BSA and 0.05% Tween 20 for 1 h. Serially diluted sera were added to the plates and incubated for 2 h at room temperature. After washing with PBS containing 0.05% Tween 20, autoantibodies were detected by HRP-conjugated goat anti-mouse IgM Ab (μ chain specific) or anti-mouse total IgG (Fcγ fragment specific; both from Bethyl Laboratories). The assays were developed by adding HRP substrate 3,3′,5,5′-tetramethylbenzidine (Vector Laboratories) and stopped by the addition of 2 N sulfuric acid. The absorbance at 450 nm was measured with a microplate reader (Spectra Max Plus; MDS Analytical Technologies). For total IgM or IgG, the concentration was calculated according to standard samples supplied by Bethyl Laboratories. For anti-dsDNA or anti-smRNP Ig, the relative amount was represented as absorbance values at the same dilutions (1:40 for IgG and 1:160 for IgM).

Histology and immunofluorescence analysis

For kidney histological analysis, both kidneys from a mouse were cut in half laterally, fixed in 10% formalin, embedded in paraffin, and stained with H&E at the Institute of Biophysics Pathology Core. The presence and severity of nephritis were evaluated in a blinded fashion, by one of the authors, with stained sections that contained glomeruli away from the medulla. Scoring of glomerulonephritis and interstitial nephritis was done using a 0 to 3 scale (0 = absent, 1 = mild, 2 = moderate, 3 = severe): scoring for glomeruli was based on glomerular size, glomerular hypercellularity, and presence of glomerular sclerosis, whereas for interstitial disease, it was based on the degree of inflammatory infiltrate and alteration in tissue architecture.

For histological analysis of the GC response, spleen samples from 5–7-mo-old mice were placed in Tissue-Tek O.C.T. compound (Sakura) and immediately frozen with a mixture of ethanol and dry ice. Cryostat sections (7 μm in thickness) were fixed in ice-cold acetone and stained with biotin-conjugated rat anti-mouse IgD (eBioscience) and FITC-conjugated anti-mouse GL-7 (BD Bioscience). HRP-conjugated extravidin (Sigma) and alkaline phosphatase–conjugated anti-FITC (Jackson ImmunoResearch) were used as secondary Abs. Enzyme reactions were developed with conventional substrates for peroxidases (diaminobenzidine/H_2O_2) and alkaline phosphatase (Fast Red; both from Sigma). Sections were counterstained with hematoxylin (Fisher).

To detect complement 3 (C3) deposition, kidneys were placed in O.C.T. compound and snap-frozen in methyl-butane chilled in liquid nitrogen. Cryostat sections (15 μm in thickness) were fixed in ice-cold acetone and stained with FITC-conjugated anti-mouse C3 (Cappel Laboratories) for 1 h at room temperature. The average intensity of FITC in the glomerular regions was quantified by ImageJ.

Flow cytometry

Splenocytes were obtained by treating the organs with digestion medium (RPMI 1640, 25 mM HEPES, 50 μg/ml Liberase [Roche] and 100 μg/ml DNase I [Worthington]). Bone marrow cells were obtained by flushing tibia and femur with medium. Kidney cells were prepared as previously described (8). Briefly, kidneys were pressed through a 70-μm cell strainer (BD Falcon). After washing, the cells were resuspended in 33% Percoll solution and centrifuged at 2000 rpm for 20 min at room temperature. Kidney-infiltrating cells were obtained from cell pellets. For staining for flow cytometry, single-cell suspensions were blocked with anti-CD16/CD32 Ab and then stained with fluorescent Abs in ice-cold flow cytometry buffer (PBS supplemented with 2 mM EDTA, 1% heat-inactivated FBS, and 0.02% sodium azide). The Abs included FITC-labeled anti-Ly6G (1A8), anti-Ly6C (HK1.4), anti-CD44 (IM7), anti–GL-7, and anti-CD43 (S7) Abs; PE-labeled anti-CD86 (GL1), anti–PD-1 (RMP1-30), anti-TCRβ (H57-597), and anti-CD23 (B3B4) Abs;

PerCP-Cy5.5–labeled anti-F4/80 (BM8), anti-ICOS (7E.17G9), and anti-IgM (RMM-1) Abs; PE-Cy7–labeled anti-CD11b (M1/70), anti-CD95 (Jo2), and anti-CD62L (MEL-14) Abs; allophycocyanin- or Alexa Fluor 647–labeled anti-CD11c (HL3), anti-CD8 (53-6.7), anti-CD138 (281-2), and anti-CD62L (MEL-14) Abs; Alexa Fluor 700–labeled anti–I-A^b (M5/114.15.2), anti-CD11b (M1/70), and anti-CD45.2 (104) Abs; allophycocyanin-Cy7–labeled anti-B220 (RA3-6B2), anti-CD19 (6D5), and Pacific Blue–labeled anti-IgD (11-26c.2a). All fluorochrome-conjugated mAbs were purchased from BD Pharmingen, eBioscience, or BioLegend. Biotinylated anti-CD86 (GL1) or anti-CD93 (AA4.1) Abs were detected with streptavidin-conjugated Pacific Orange (Invitrogen). After the final wash, the cells were resuspended in flow cytometry buffer containing 0.4 μM DAPI (Invitrogen). All data were collected on an LSR II flow cytometer (Becton Dickinson) and analyzed with FlowJo software (TreeStar).

Immature, transitional, and mature B cell populations were identified in the spleen and bone marrow of mice using fluorescently conjugated Abs against surface B220, CD23 (BD Biosciences), CD93 (clone AA4.1; eBioscience), and IgM F(ab)′ monomer (Jackson ImmunoResearch). In the spleen, surface CD93 was used to distinguish immature (B220$^+$, CD93$^+$) and mature (B220$^+$, CD93$^-$) B cells. Within the immature B cell population, surface CD23 and IgM levels were used to identify immature-transitional T1 (IgM^{hi}, CD23$^{lo\text{-}neg}$), T2 (IgM^{hi}, CD23$^{hi\text{-}int}$), and T3 (IgM^{lo}, CD23$^{hi\text{-}int}$) subsets. Within the mature B cell population, surface expression of CD23, CD21, IgM, and CD43 were used to distinguish follicular B cells (CD23$^+$, CD21^{lo}, IgM$^{lo\text{-}int}$), marginal zone B cells (CD23$^{lo\text{-}neg}$, CD21^{hi}, IgM^{hi}, CD43$^-$), and B1 B cells (CD23$^{lo\text{-}neg}$, CD21$^{neg\text{-}lo}$, IgM^{lo}, CD43$^+$). These markers were also used to distinguish immature and pro/pre-B cells (B220$^+$, CD93$^+$) and mature recirculating B cells (B220$^+$ CD93$^-$) in the bone marrow. Surface IgM and CD23 levels within the CD93$^+$ population distinguish newly formed immature B cells (IgM$^+$, CD23$^{lo\text{-}neg}$), BM-T1 cells (IgM^{hi}, CD23$^{lo\text{-}neg}$), BM-T2 cells (IgM^{hi}, CD23^{int}), and pro/pre-B cells (IgM$^-$, CD23$^-$). Absolute cell numbers within each population were back-calculated from total splenocytes or total cells/femur and tibia.

RNA extraction and quantitative RT-PCR

For quantifying cytokine expression, mouse spleens were harvested and snap-frozen in liquid nitrogen. Total RNA was extracted with the RNeasy kit (QIAGEN) with on-column DNase digestion. cDNA was transcribed from total RNA with the iScript cDNA Synthesis Kit (Bio-Rad). The primer pairs for IL-12p40, IL-6, and BAFF were described previously (8). Transcripts were quantified by PCR with iTaq SYBR Green SuperMix with ROX (Bio-Rad), and the levels of cytokine transcripts were normalized to the levels of HPRT mRNA.

Statistical analysis

Statistical significance for data with multiple groups was calculated with a one-way ANOVA; if a significant difference was observed between groups, the Bonferroni posttest was used to assess the statistical difference between specific groups and either the wild-type (WT) group or the *Lyn*$^{-/-}$ group. In cases in which there was a large difference between the WT group and the three groups with Lyn deficiency (B cell number data, Fig. 3E, Fig. 6B, Supplemental Fig. 1B), this analysis was inadequate to detect differences between the Lyn-deficiency groups, because all were greatly different from the WT group. In these cases, a secondary statistical analysis was performed with just the Lyn-deficiency groups. In the figures, this secondary statistical analysis is denoted by different symbols. When there were three such groups, this secondary analysis again used one-way ANOVA; however, in cases in which only two groups remained, the Mann–Whitney *U* test was used. All p values ≤ 0.05 were considered significant and are indicated in the figures.

Results

Ablation of MyD88 signaling in either B cells or DCs attenuates autoimmunity in Lyn$^{-/-}$ *mice*

To examine the contribution of TLR signaling in B cells and DCs to the spontaneous autoimmunity caused by Lyn deficiency, mice with a conditional allele of *Myd88* (*Myd88*^{fl}) were crossed to *Lyn*$^{-/-}$ mice, and transgenic Cre alleles that express selectively in B cells (*Cd79a-Cre*) or in DCs (*CD11c-Cre*) were also introduced. Progenies of genotypes *Lyn*$^{-/-}$ *Myd88*$^{fl/fl}$, *Lyn*$^{-/-}$ *Myd88*$^{fl/fl}$ *Cd79a-Cre*, or *Lyn*$^{-/-}$ *Myd88*$^{fl/fl}$ *Cd11c-Cre* (hereafter referred to as *Lyn*$^{-/-}$, *Lyn*$^{-/-}$ *B-Myd88*$^{-/-}$, and *Lyn*$^{-/-}$ *DC-Myd88*$^{-/-}$ mice, respectively) were generated, housed under specific pathogen–free conditions, and examined for autoimmune phenotypes at different ages.

The development of autoantibodies by these mice was initially screened by ANA immunofluorescence, with mouse sera collected at 5–7 mo of age. As previously described (4, 5), most *Lyn*$^{-/-}$ mice exhibited elevated titers of ANAs by this age (Fig. 1A, 1B). The development of IgG ANAs was almost completely abolished in *Lyn*$^{-/-}$ *B-Myd88*$^{-/-}$ mice, and it was substantially attenuated in mice lacking MyD88 selectively in DCs (Fig. 1A, 1B).

Next, we used ELISA to examine the development of Abs to dsDNA and smRNP, two major types of ANAs seen in SLE patients (1), as well as in animal models of SLE. All *Lyn*$^{-/-}$ mice developed IgM autoantibodies against both of these nuclear Ags, typically by 4 mo of age, and a substantial majority also developed IgG anti-dsDNA and IgG anti-smRNP. Deletion of MyD88 in DCs delayed production of these autoantibodies, but 8–10-mo-old mice still had substantial titers of IgG and IgM anti-dsDNA and IgM anti-smRNP. In contrast, deletion of *Myd88* in B cells prevented the production of IgG autoantibodies in *Lyn*$^{-/-}$ *B-Myd88*$^{-/-}$ mice at all time points tested and attenuated the production of IgM autoantibodies (Fig. 1C–F). Total serum IgM and IgG levels were somewhat reduced in these mice compared with *Lyn*$^{-/-}$ mice (Fig. 1G, 1H), but the differences were generally ≤2-fold, indicating that there was a selective defect in the production of autoantibodies.

Anti-dsDNA IgG Abs are often deposited in the glomeruli of the kidneys and can lead to glomerulonephritis, as observed in Lyn-deficient mice (8, 31). Indeed, immunofluorescent staining clearly revealed a large amount of C3 deposition in the glomeruli of most of the 5–7-mo-old *Lyn*$^{-/-}$ mice (Fig. 2A, 2B). In agreement with the almost complete abolishment of IgG autoantibodies in *Lyn*$^{-/-}$ *B-Myd88*$^{-/-}$ mice, C3 deposition was not evident in the glomeruli of these mice at a corresponding age. Moreover, the nephritis typically seen in old *Lyn*$^{-/-}$ mice by H&E staining of kidney tissue sections was substantially decreased, but not completely absent, in Lyn-deficient mice deleted for MyD88 in either B cells or DCs (Fig. 2C, 2D); the numbers of infiltrating inflammatory cells (CD45$^+$), mainly CD11b$^+$ neutrophils and macrophages, were correspondingly reduced (Fig. 2E). The splenomegaly and myeloproliferation that are characteristic of aged *Lyn*$^{-/-}$ mice (>6 mo old) were corrected by deletion of *Myd88* in DCs but apparently not by deletion of *Myd88* in B cells (Fig. 3A, 3B, Supplemental Fig. 1A). Together, these results are consistent with the observation that ablating MyD88 signaling in B cells or DCs reduces IgG autoantibody production in *Lyn*$^{-/-}$ mice but also indicates that some of the inflammatory phenotypes are independent of autoantibody production.

Autoantibody production in Lyn$^{-/-}$ *mice requires SAP expression and T cell help*

Abs against dsDNA obtained from MRL/*lpr* mice exhibit somatic mutations that increase reactivity to DNA (32), which is consistent with a GC origin for these autoantibody responses. However, Ig-transgenic B cells with a rheumatoid factor specificity in these mice make an extrafollicular Ab response with substantial numbers of somatic mutations, even in the absence of Ag-specific T cell help (21, 33). Moreover, mice overexpressing BAFF also spontaneously produce ANAs in a T cell–independent fashion (34). Thus, there are precedents for extrafollicular production of ANAs in some mouse models.

To address this issue, we first examined *Lyn*$^{-/-}$ mice for the frequency of GC phenotype B cells. The frequency of CD95$^+$GL-7$^+$ GC B cells relative to the number of splenic B cells already was significantly increased in *Lyn*$^{-/-}$ mice compared with WT mice

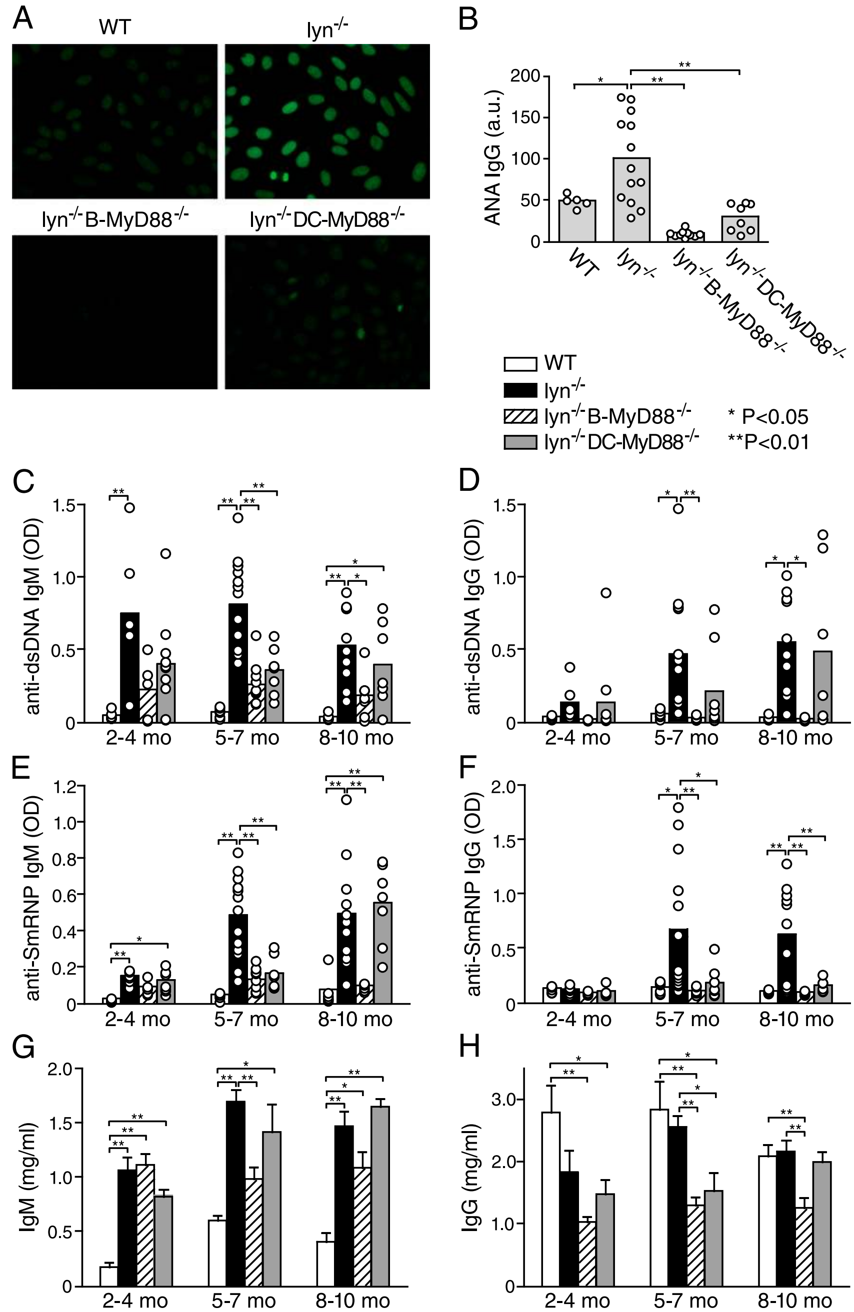

FIGURE 1. Roles of MyD88 signaling in B cells and in DCs for development of autoantibodies in *Lyn*$^{-/-}$ mice. (**A** and **B**) Anti-nuclear IgG Abs of individual mice were screened using sera of 5–7-mo-old mice. Representative ANA fluorescence images (original magnification ×40) of 1:40 diluted sera of the indicated genotype (A), as well as summarized relative fluorescence intensity of sera from individual mice (○) and means of each mouse group (bars) (B). Serum IgM and IgG Abs to dsDNA (**C**, **D**) and to anti-smRNP (**E**, **F**) of individual mice of the four genotypes indicated and of different age groups were measured by ELISA. The relative amount of autoantibody in each mouse (○) and the mean of each mouse group (bars) are shown. (**G** and **H**) Total serum IgM and IgG levels of mice of the different genotypes and age groups were quantified by ELISA. Data are presented as mean ± SE of WT (n = 6, 6, 6 mice, respectively, in each age group), *Lyn*$^{-/-}$ (n = 6, 13, 11), *Lyn*$^{-/-}$ *B-MyD88*$^{-/-}$ (n = 6, 10, 7), and *Lyn*$^{-/-}$ *DC-MyD88*$^{-/-}$ (n = 7, 8, 7) mice. Differences between WT or *Lyn*$^{-/-}$ and other groups are indicated by brackets. *$p < 0.05$, **$p < 0.01$.

by 2–4 mo, and this increase became more dramatic at 5–7 mo (Fig. 3C, 3D), correlating with the time course of the development of IgG ANAs. However, it should be noted that *Lyn*$^{-/-}$ mice have substantially fewer splenic B cells than do WT mice (Supplemental Fig. 1B), so the absolute numbers of GC B cells were similar in *Lyn*$^{-/-}$ mice and WT mice (Fig. 3E). In agreement with flow cytometry analysis, staining of spleen sections also clearly revealed the existence of IgD^{low}GL-7^{+} GC structures in multiple follicles of *Lyn*$^{-/-}$ mice (Fig. 3F) at 5–7 mo of age. In contrast, GCs were not common in WT mice housed in the same mouse room (data not shown). Interestingly, the spontaneous GC response seen in *Lyn*$^{-/-}$ mice was greatly reduced upon deletion of *Myd88* in B cells (Fig. 3D, 3E). In contrast, the mesenteric lymph nodes of *Lyn*$^{-/-}$ and *Lyn*$^{-/-}$ *B-Myd88*$^{-/-}$ mice contained similar numbers of GC B cells (data not shown), suggesting that the latter mice did not have a general defect in mounting GC reactions.

To examine whether Th cells and the GC reaction contribute to the generation of IgG ANAs, we crossed *Lyn*$^{-/-}$ mice to mice deleted for TCR genes (*tcrβ*$^{-/-}$ *tcrδ*$^{-/-}$) or to mice lacking the SAP signaling adaptor protein, which is critical for follicular helper T (Tfh) cells to interact with GC B cells and promote GC Ab responses (35, 36). Lyn-deficient mice lacking T cells or lacking the SAP adaptor molecule made greatly attenuated levels of anti-dsDNA IgG Abs, as measured by ELISA (Fig. 3G). These genetic results strongly support the hypothesis that there is a GC-origin of lupus-like autoantibodies in Lyn-deficient mice.

Activation and expansion of self-reactive T cells in Lyn$^{-/-}$ *mice require MyD88 signaling in DCs and B cells*

Lyn$^{-/-}$ mice exhibit a dramatic expansion of activated T cells as autoimmune disease progresses (8, 37). Therefore, we next investigated the role of MyD88 in DCs and B cells in the hyperreactivity of T cells in *Lyn*$^{-/-}$ mice. As previously reported (8), *Lyn*$^{-/-}$ mice accumulate increasing numbers of CD4^{+} and CD8^{+} T cells with an activated or effector memory phenotype (CD44^{+} CD62L^{low}) as they age. As Lyn-deficient mice lacking MyD88 in

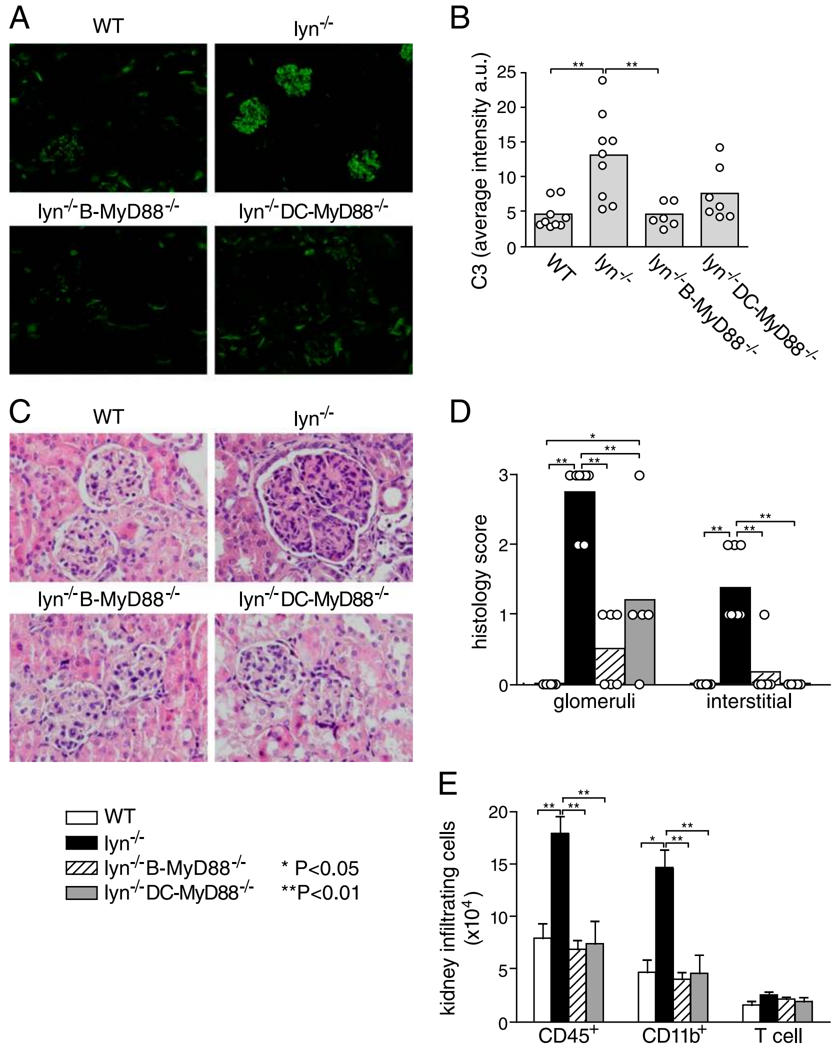

FIGURE 2. Effect of ablation of MyD88 signaling in B cells and in DCs for complement deposition and inflammation in the kidneys of *Lyn*$^{-/-}$ mice. Deposition of C3 was detected by immunofluorescent staining of frozen kidney sections of 5–7-mo-old mice of the indicated genotype; representative images (original magnification ×20) (**A**) and summarized data (**B**) are shown. (**C**) Kidney sections of the different genotypes at 8–10 mo of age were stained with H&E to assess pathological changes associated with glomerulonephritis (original magnification ×40). (**D**) Sections from individual mice were graded, in a blinded fashion, on a scale of 0 to 3 (0 = absent, 1 = mild, 2 = moderate, 3 = severe) for the degree of histological abnormality in the glomeruli and for the degree of inflammation in the interstitial regions. (**E**) Numbers of inflammatory cells in the kidneys were measured by flow cytometry in six mice of each genotype at 8–10 mo of age. Data are mean ± SE and are representative of two separate experiments. $^*p < 0.05$, $^{**}p < 0.01$.

B cells or in DCs aged, these populations did not increase at all (CD4$^+$ T cells) or nearly as much (CD8$^+$ T cells) (Fig. 4A–C, Supplemental Fig. 1C, 1D). Thus, increased spontaneous activation of T cells in *Lyn*$^{-/-}$ mice was largely dependent on MyD88 signaling in both DCs and B cells.

Many of the activated CD4$^+$ T cells also expressed ICOS and PD-1, two markers that have been used to identify Tfh cells. The percentage and absolute number of those cells already were slightly elevated in *Lyn*$^{-/-}$ mice at 2–4 mo of age compared with WT mice, and they especially increased in older mice (Fig. 4E, 4F). In another recent study (38), the number of Tfh cells at 4–5 mo of age was roughly normal in *Lyn*$^{-/-}$ mice. Importantly, deletion of *Myd88* in either DCs or B cells substantially reduced the expansion of these cells in *Lyn*$^{-/-}$ mice (Fig. 4E, 4F).

Splenic B cells and DCs in Lyn$^{-/-}$ *mice have elevated expression of MHC class II and CD86 that is not dependent on MyD88 signaling*

TLR agonists have well-established adjuvant properties for promoting T cell responses (39). To investigate the possibility that TLRs of DCs or B cells promote their ability to present self-Ags to T cells, we examined the expression of MHC class II and of the costimulatory molecule CD86 on splenic B cells and on DCs of *Lyn*$^{-/-}$ mice with or without DC or B cell MyD88. In *Lyn*$^{-/-}$ mice, an increased proportion of B cells exhibited elevated levels of MHC class II and CD86 by 2–4 mo of age (Fig. 5A, 5B). The number of such B cells was not dependent on the expression of MyD88 in B cells (Fig. 5A, 5B), suggesting that the loss of Lyn-based attenuation of BCR signaling in B cells may be sufficient for this phenotypic alteration. Similarly, DCs in young *Lyn*$^{-/-}$ mice had spontaneously elevated MHC class II expression and CD86 expression. Deletion of *Myd88* in DCs had little effect on their expression of MHC class II and CD86 (Fig. 5C, 5D). Together, these data indicate that the requirement for MyD88 in B cells and in DCs for development of autoimmunity in *Lyn*$^{-/-}$ mice was not caused by changes in the expression of MHC class II and CD86.

Next, we examined the role of MyD88 signaling in DCs and B cells in *Lyn*$^{-/-}$ mice for the induction of cytokines that have been implicated in the pathogenesis of autoimmunity and inflammation in this model (8, 40). In total splenocytes from *Lyn*$^{-/-}$ mice at 2 mo of age, increased mRNA expression of the cytokines IL-12p40 and BAFF was readily detected (Fig. 5E–G), demonstrating that enhanced inflammatory responses arise even before the development of overt autoimmunity in these mice. Interestingly, deletion of *Myd88* in DCs substantially reduced the expression of IL-12p40 and IL-6 in the spleens of young *Lyn*$^{-/-}$ mice (Fig. 5E, 5F), suggesting that Lyn-deficient DCs are sensitized to have enhanced responses to endogenous or ubiquitous TLR ligands and are a major producer of proinflammatory cytokines in these mice. This is in agreement with other recent reports (10, 11) describing a proinflammatory role for Lyn-deficient DCs. As mentioned above, the incidence of splenomegaly was greatly reduced in aged (8–10 mo) *Lyn*$^{-/-}$ *DC-MyD88*$^{-/-}$ mice compared with *Lyn*$^{-/-}$ mice (Fig. 3A, 3B). In comparison, deletion of

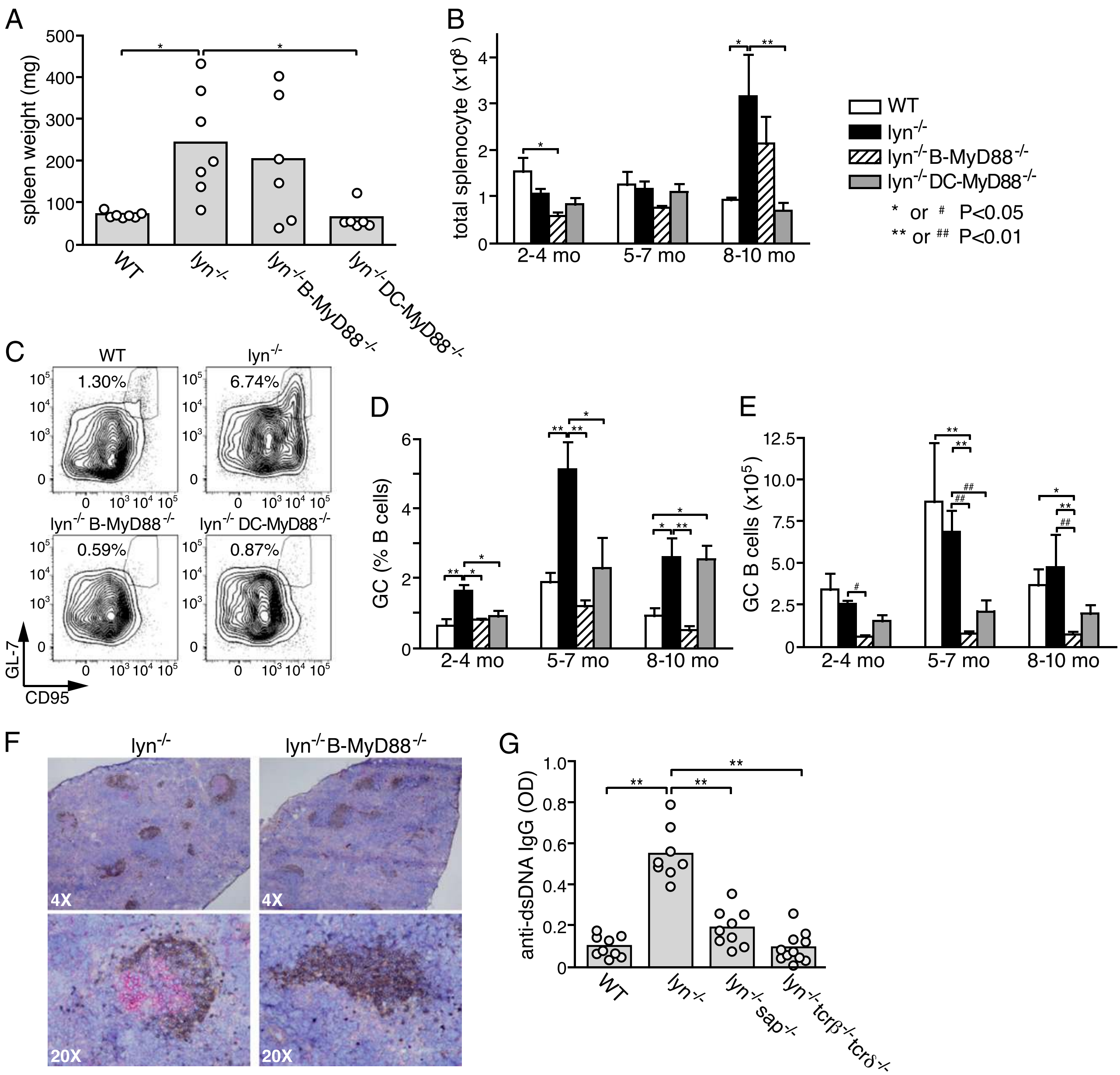

FIGURE 3. Role of GC response in autoantibody production by *Lyn*$^{-/-}$ mice and effect of ablation of MyD88 on GCs. Effect of deletion of *Myd88* in B cells or DCs for the splenic hypercellularity that accumulates over time in Lyn-deficient mice; spleen weights of individual mice at 8–10 mo of age for the indicated genotypes (**A**) and numbers of total splenocytes (mean ± SE) for mice of different ages (**B**). Analysis of GC B cells; representative flow cytometry profiles (**C**) and summarized data from mice with different genotypes and at different ages, represented either as percentage of total splenic B cells that have a GC B cell phenotype (**D**) or as absolute number of GC B cells/spleen in the indicated mice (**E**). Data in (D) and (E) are mean ± SE of five to eight mice/group and are representative of three separate experiments. (**F**) Representative immunohistological staining of GCs in the spleens of 5–7-mo-old *Lyn*$^{-/-}$ and *Lyn*$^{-/-}$ *B-MyD88*$^{-/-}$ mice. IgD^{+} cells (brown) and GL-7^{+} cells (red) are shown with hematoxylin counterstaining (original magnification ×4 or ×20, as indicated). (**G**) Effect of genetic deletion of T cells or the adaptor molecule SAP on ANA production of *Lyn*$^{-/-}$ mice at 5–6 mo of age. Shown are the relative amounts of anti-dsDNA IgG measured by ELISA in individual mice (○) and means of each mouse group (bars). $^{*}p < 0.05$, $^{**}p < 0.01$, ANOVA, as described in *Materials and Methods*. A secondary statistical analysis in which the WT group was excluded was also performed on the data in (E). $^{\#}p < 0.05$, $^{\#\#}p < 0.01$.

B cell *Myd88* had little or no effect on the expression of IL-12p40 or BAFF (Fig. 5E–G).

Effect of cell-intrinsic MyD88 signaling on peripheral numbers of B cells in Lyn$^{-/-}$ *mice*

Lyn deficiency has substantial B cell–intrinsic effects on the numbers of B cells in the spleen (8), decreasing their overall numbers (Supplemental Fig. 1B), apparently as a result of enhanced cell death at the T1 or T2 immature stages in the spleen and decreased maturation to the follicular mature state and/or decreased survival of these cells (41–43). Interestingly, although deletion of *Myd88* in *Lyn*$^{-/-}$ B cells did not affect bone marrow populations of B cell precursors or immature B cells compared with *Lyn*$^{-/-}$ mice (Fig. 6A), the decreased number of B cells in the spleens of young *Lyn*$^{-/-}$ mice was further exacerbated by deletion of *Myd88* in B cells (Fig. 6B). The reduction in B cells in *Lyn*$^{-/-}$*B-Myd88*$^{-/-}$ mice began at the T1 stage in the spleen and persisted in subsequent developmental stages until maturation (Fig. 6B, 6C). Despite these decreases in mature B cell number, the numbers of plasma cells in the spleen were elevated in *Lyn*$^{-/-}$ and *Lyn*$^{-/-}$*B-Myd88*$^{-/-}$ mice compared with WT mice

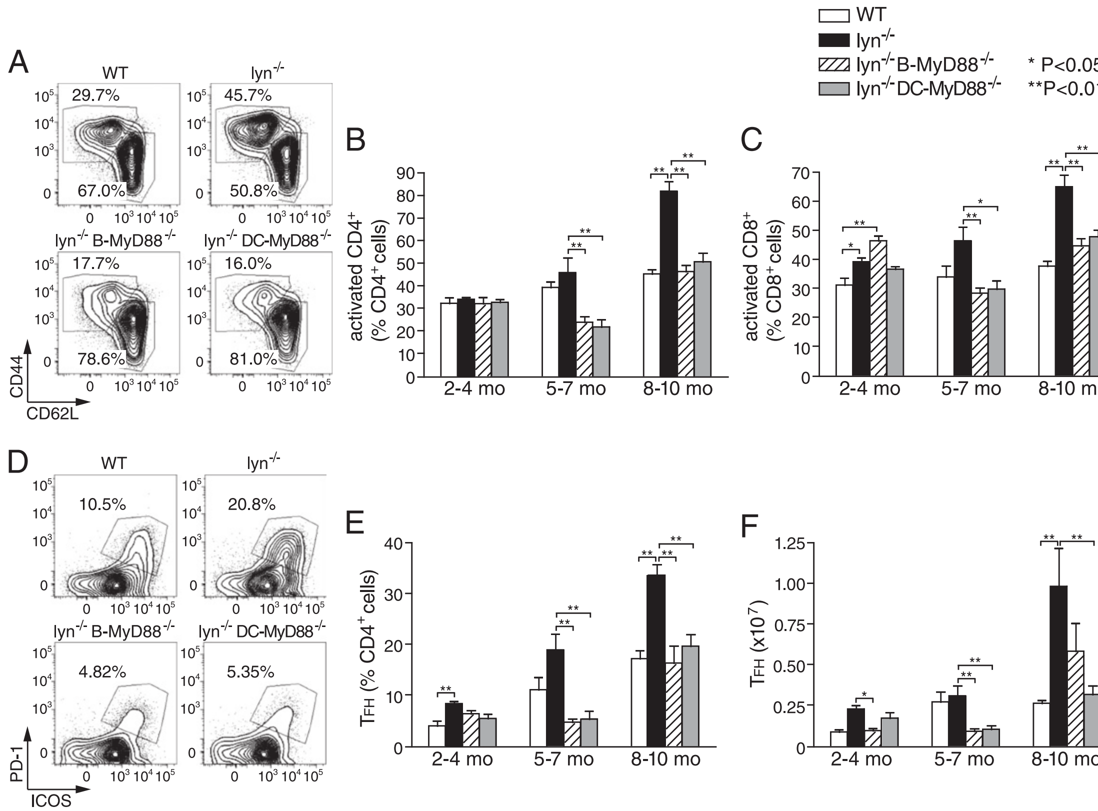

FIGURE 4. Roles of MyD88 signaling in DCs and B cells for the activation and expansion of T cells in *Lyn*$^{-/-}$ mice. (**A**–**C**) Age-dependent accumulation of activated phenotype T cells in *Lyn*$^{-/-}$ mice and effect of ablation of *Myd88* in B cells or DCs. Representative flow cytometry plots of activated CD4$^+$ T cells (CD44^{hi} CD62L^{low}) in spleens of 5–7-mo-old mice of the indicated genotype (A) and summarized data for CD4$^+$ T cells (B) and CD8$^+$ T cells (C) from mice of different ages. (**D**–**F**) Age-dependent accumulation of Tfh phenotype cells in *Lyn*$^{-/-}$ mice. Representative flow cytometry plots of Tfh cells (PD-1$^+$ ICOS$^+$) for gated CD4$^+$ T cells in the spleen (D) and summarized data (E, F). Data in (B), (C), (E), and (F) are mean ± SE (n = 5–8 mice/group) and are representative of three separate experiments. *$p < 0.05$, **$p < 0.01$.

(Supplemental Fig. 1E). These results suggest that MyD88 signaling in B cells promotes their survival at the immature T1 stage in the spleen, but it does not greatly affect maturation or survival at subsequent stages of development in the spleen and is not required for differentiation into plasma cells, in agreement with the circulating levels of total IgM and IgG in these mice (Fig. 1G, 1H). We observed a modest increase in the percentage of CD93$^+$CD23$^+$IgM^{low} T3 B cells and a small decrease in the percentage of follicular B cells in the spleens of *Lyn*$^{-/-}$*B-Myd88*$^{-/-}$ mice, such that the ratio of T3/follicular B cells was slightly, but significantly, increased by the loss of MyD88 in B cells (Fig. 6D). The T3 B cell population previously was shown to include many anergic autoreactive B cells (44). Our data suggest that intrinsic MyD88 signaling may keep some self-reactive B cells from becoming anergic, although other explanations are possible.

Discussion

Lyn is an intracellular protein tyrosine kinase that is critical for inhibitory receptor function in B cells and in DCs, and *Lyn*$^{-/-}$ mice spontaneously develop a lupus-like autoimmune and inflammatory disease (4, 5). To address the mechanism by which nucleic acid–recognizing TLRs contribute to spontaneous production of ANAs in the *Lyn*$^{-/-}$ mouse model of SLE, we used cell type–specific deletion of the gene encoding MyD88, a key adaptor molecule required for intracellular signaling by most TLRs, including TLR7 and TLR9. Deletion of *Myd88* selectively in B cells completely blocked production of the anti-dsDNA and anti-RNP IgG Abs, which are among the most characteristic autoantibodies seen in human SLE and are rarely produced in other human diseases (1), and ameliorated glomerulonephritis. In addition, deletion of *Myd88* selectively in DCs delayed production of IgG anti-dsDNA, blocked production of IgG anti-smRNP, largely abrogated accumulation of activated phenotype T cells in the spleen, and ameliorated glomerulonephritis. These results demonstrate that TLR/MyD88 signaling is required in both B cells and DCs for the development of autoimmune disease in these mice.

The demonstration that MyD88/TLR signaling in B cells is required for anti-nuclear IgG production in *Lyn*$^{-/-}$ mice adds to the accumulating evidence indicating that dual stimulation of DNA- and RNP-specific B cells by the BCR and by TLR9 or TLR7, respectively, is a key underlying mechanism in the breakdown of tolerance to nuclear self-Ags in mouse models of lupus (15, 45, 46). Although TLR signaling can boost Ab responses in multiple ways (47), we recently showed that it can boost GC responses dramatically in response to virus-like particles and inactivated virions (24). It is likely that an analogous mechanism, perhaps in response to fragments from apoptotic cells, participates in the production of anti-dsDNA and anti-RNP IgG Abs in *Lyn*$^{-/-}$ mice, because it was largely dependent on MyD88 expression in B cells, on the presence of T cells, and on the expression of SAP, which is required for GC responses (Fig. 3G). SAP is an adaptor for SLAM family adhesion molecules, and its function in T cells is important at early stages of the GC response by acting to stabilize interactions between activated B cells and cognate Th cells (36). Moreover, a recent report from another group (38) found that *Lyn*$^{-/-}$ *IL-21*$^{-/-}$ mice failed to produce anti-dsDNA IgG Abs, which is also consistent with an

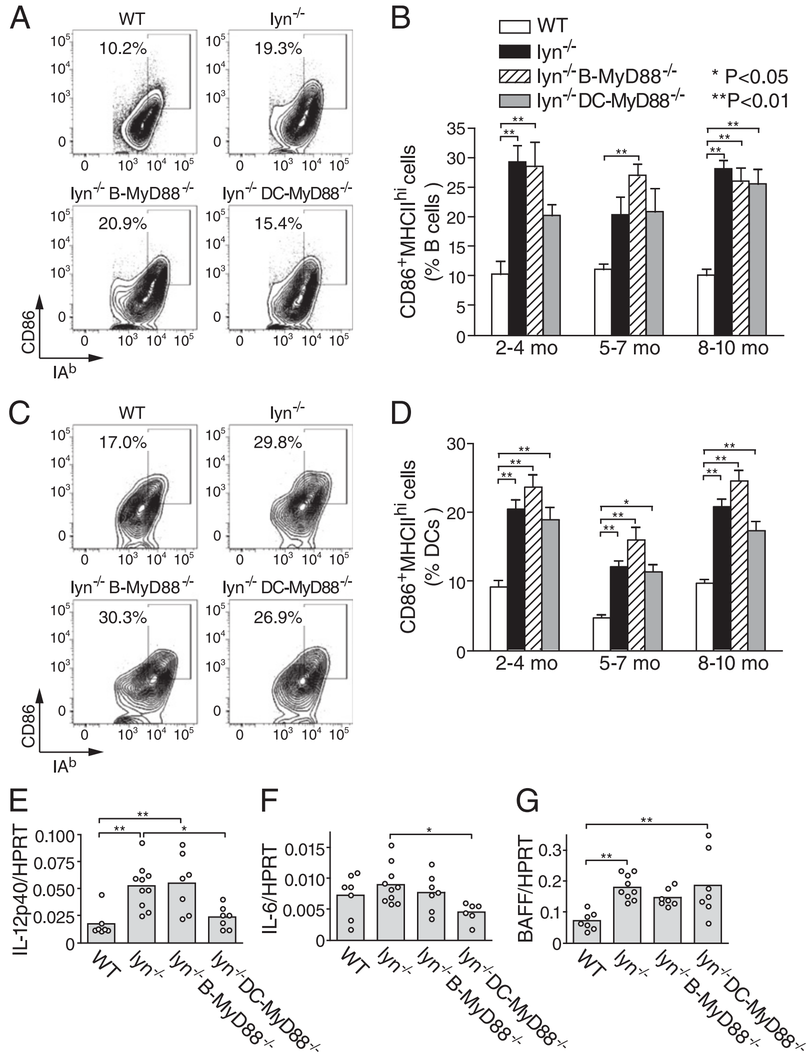

FIGURE 5. Role of MyD88 signaling for the activation of B cells and DCs in *Lyn*$^{-/-}$ mice. (**A** and **B**) Characterization of the fraction of splenic B cells with an activated phenotype in *Lyn*$^{-/-}$ mice. Representative flow cytometry plots examining the expression of MHC class II and CD86 on gated CD19$^+$ B cells in the spleen (A) and summary data for the percentage of B cells in the spleen with an activated MHC II$^+$ CD86$^+$ phenotype (B). (**C** and **D**) Characterization of the fraction of DCs in the spleen with an activated phenotype. Representative flow cytometry plots for characterization of activated phenotype of splenic DCs gated on CD11c^{hi} MHC II$^+$ cells (C) and summary data for the percentage of DCs in the spleen with an activated MHC II$^+$ CD86$^+$ phenotype (D). Data in (B) and (D) are mean ± SE (n = 5–8 mice/mouse group) and are representative of three separate experiments. Expression of IL-12p40 (**E**), IL-6 (**F**), and BAFF (**G**) mRNAs in total splenocytes from 2-mo-old mice were quantified by real-time PCR. Data of each mouse (○) and the mean of each mouse group (bars) are presented as relative abundance of each cytokine mRNA normalized to HPRT mRNA. *$p < 0.05$, **$p < 0.01$.

important role for the GC response in the production of these Abs, given the known role of IL-21 in the GC response. Curiously, in that study, glomerulonephritis was not ameliorated despite a substantial decrease in most IgG autoantibodies. Thus, a number of results strongly implicate the GC response in the production of anti-nuclear IgG Abs in Lyn-deficient mice.

Our finding of a requirement for T cells in the autoimmunity of *Lyn*$^{-/-}$ mice is consistent with previous data demonstrating that the T cell production of IFN-γ plays a critical role in the autoimmune phenomena of Lyn-deficient mice (8) and that IL-10 from B cells decreases the inflammatory reaction generated by T cells in these mice (9). Interestingly, a previous study (48) found that CTLA4-Ig blockade of T cell costimulation via CD28 prevented IgG ANAs production but there was now production of IgA. The mechanism of IgA ANA production in these treated mice is unclear at this time.

The GC response has been implicated in lupus-like autoantibody production in several other mouse models of SLE, including the NZB × NZW F1 mouse (46, 49, 50). However, it should be noted that autoantibody production occurs independently of T cells in BAFF-overexpressing transgenic mice (34), or in MRL/lpr mice expressing a rheumatoid factor Ig transgene (21). Therefore, the nature of the genetic alterations causing susceptibility to SLE apparently can affect, to some degree, the underlying immunological mechanism of autoantibody production. These results suggest that human SLE may also be mechanistically diverse; therefore, it will be of interest to develop methods for analyzing immune cells from SLE patients to assess such possible heterogeneity because this may be relevant to their treatment.

In previous studies (24) of the role of MyD88 signaling in B cells versus DCs for Ab responses to Ag–CpG oligonucleotide conjugates, we found that the cellular requirement for an optimal IgG response to the Ag depended on the physical form of the Ag. When soluble protein Ags, such as OVA or the ragweed pollen Ag Amb a1, were used, MyD88 in DCs was required, and MyD88 in B cells did not contribute to the response. In contrast, when virus-like particles containing TLR9 or TLR7 ligands or chemically inactivated influenza virus particles were used as immunogen, the IgG response to viral coat proteins was greatly augmented by MyD88 signaling in B cells but not by MyD88 signaling in DCs. Moreover, for virus-like particles, the magnitude of the TLR effect was dependent on the epitope density of the Ag on the particle, indicating that stronger BCR signaling enabled TLR7 or TLR9 in B cells to enhance the response (24). This enhancement occurred by promotion of the GC component of the response (24). Conversely, weak BCR signaling, as likely occurs with the soluble protein Ags, did not enable B cell TLR9 to boost the IgG response. Based on the results obtained in this study and the results obtained previously, we propose that the true autoantigen in SLE is a particulate form of chromatin and/or RNPs, such as occurs on

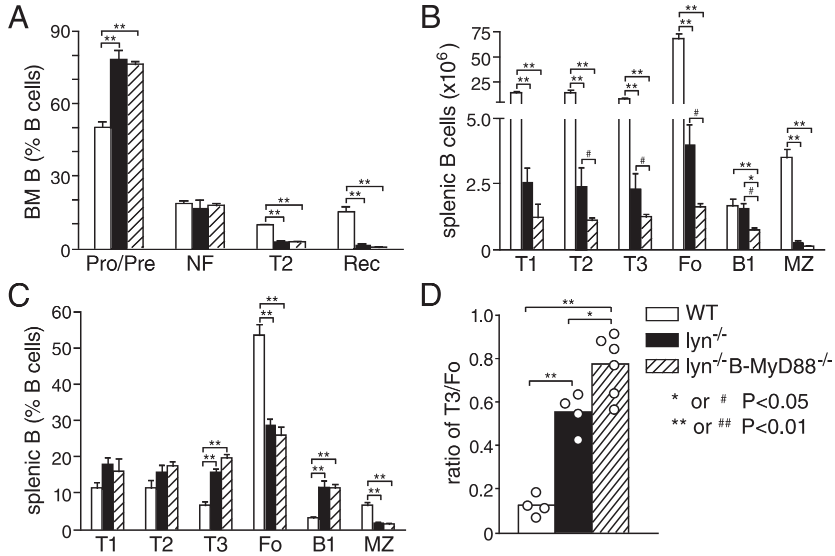

FIGURE 6. Effect of cell-intrinsic MyD88 signaling on B cell development in *Lyn*$^{-/-}$ mice. Effect of ablation of *Myd88* in B cells for the numbers of B cell precursors, immature B cells, and mature B cells in the bone marrow (**A**) or spleen (**B**, **C**) of 2–4-mo-old *Lyn*$^{-/-}$ mice. Also shown for comparison purposes are B cell populations from WT mice. (A) Percentage of bone marrow cells that were CD19$^+$CD93$^+$IgM$^-$ pro- and pre-B (Pro/Pre), CD19$^+$CD93$^+$IgM$^+$CD23$^-$ newly formed immature B cells, CD19$^+$CD93$^+$IgM$^+$CD23$^+$ T2 B (T2), and CD19$^+$CD93$^-$IgM$^+$CD23$^+$ recirculating B cells. Also shown are the absolute numbers (B) and percentage (C) of CD19$^+$CD93$^+$IgM$^+$CD23$^-$ T1 B (T1), CD19$^+$CD93$^+$IgM^{hi}CD23$^+$ T2 B (T2), CD19$^+$CD93$^+$IgM^{low}CD23$^+$ T3 B (T3), CD19$^+$CD93$^-$IgM$^+$CD23$^+$ follicular B (Fo), CD19$^+$CD23$^{lo\text{-}neg}$CD21^{hi}IgM^{hi}CD43$^-$ marginal zone (MZ), and CD19$^+$CD93$^-$CD23$^-$ CD21$^{lo\text{-}neg}$CD43$^+$B1 B cells (B1) in the spleens. (**D**) Ratio of T3 B cells/follicular B cells in the spleens of *Lyn*$^{-/-}$ and *Lyn*$^{-/-}$ *B-Myd88*$^{-/-}$ mice. Data are mean ± SE (n = 4–6 mice/group) and are representative of three separate experiments. $*p < 0.05$, $**p < 0.01$, ANOVA. As described in *Materials and Methods*, a secondary statistical analysis in which the WT group was excluded was also performed on the data in (B): $^{\#}p < 0.05$, $^{\#\#}p < 0.01$.

apoptotic fragments released from dying cells. This proposal is consistent with the fact that many autoantibodies obtained from mouse SLE-prone strains bind to apoptotic blebs (51).

The observation mentioned above—that strong BCR signaling is required to enable TLR7 or TLR9 signaling in B cells to enhance their GC response—suggests why Lyn deficiency of B cells creates a strong susceptibility for the development of anti-dsDNA and anti-RNP IgG Abs. Low-affinity DNA- or RNP-reactive mature or anergic follicular B cells in WT mice presumably have weak BCR signaling that is attenuated by the Lyn/CD22/SHP-1 feedback-inhibitory pathway; therefore, even if they acutely encounter apoptotic blebs, their low level of BCR signaling does not synergize with TLR7 or TLR9 signaling to promote a GC response. In contrast, Lyn-deficient B cells of the same specificity have exaggerated BCR signaling; therefore, we hypothesize that they can enter into and participate in GC responses, leading to the production of class-switched and affinity-matured pathogenic autoantibodies.

Several recent studies (10, 11) implicated dysregulation of DCs by loss of Lyn as also being an important contributor to the autoimmune phenomena in *Lyn*$^{-/-}$ mice. Consistent with this view is our demonstration that MyD88 signaling in DCs contributes importantly to the autoimmune phenotypes of *Lyn*$^{-/-}$ mice. The characteristic expansion of activated phenotype T cells that is seen in *Lyn*$^{-/-}$ mice as they get older was abrogated by deletion of *Myd88* in DCs (Fig. 4), indicating that TLR/MyD88 signaling in DCs provides a necessary activation signal that synergizes with the effects of loss of Lyn-dependent inhibitory signaling in these cells. This interpretation is supported by the recent report (11) that mice in which Lyn is deleted only in DCs also develop a severe lupus-like autoimmunity. Thus, we propose that *Lyn*$^{-/-}$ mice develop a severe lupus-like autoimmunity and inflammatory disease as a result of the combination of at least two defects: the deficiency of Lyn in B cells compromises their cell-intrinsic tolerance mechanisms by allowing TLR7 and TLR9 to promote activation of self DNA- and RNP-reactive B cells, and the dysregulation of Lyn-deficient DCs leads to excessive activation of T cells, which, in turn, can promote increased affinity IgG responses of the DNA- and RNP-specific B cells. In addition, Lyn-deficient DCs and the T cells activated by them provide a self-reinforcing inflammatory response that can also contribute to inflammatory disease (8, 11). This latter component of the disease of Lyn-deficient mice is especially evident if Lyn is selectively deleted in DCs (11) or if the B cells are unable to produce IL-10 to inhibit it (9).

Studies in mouse models indicate that the presence of genetic susceptibility loci is required for spontaneous breakdown of tolerance to nuclear autoantigens. Although most natural susceptibility loci in human and mouse remain poorly understood, a subset of identified loci alters regulation of BCR signaling, including ablation of Lyn (4, 31), B cell–specific deletion of SHP-1 (52), deletion of CD22 (53), and a point mutation of CD45 that increases the activity of some Src family tyrosine kinases while decreasing the activity of Lyn (54, 55). Strikingly, Lyn, CD22, and SHP-1 work together in a feedback-inhibitory pathway to limit BCR signaling, especially in mature B cells (4, 56). Genetic analysis in human SLE patients suggests that this pathway is likely compromised in some SLE patients (12, 13). Thus, the *Lyn*$^{-/-}$ mouse model of lupus is highly relevant to a subset of human SLE patients. Our results indicate that TLR/MyD88 signaling is likely to be necessary for ANA production in this subset of patients.

Acknowledgments

We thank Derek Rookhuizen for helpful discussions related to analysis of Tfh cells by flow cytometry and Yongmei Hu for assistance with animal husbandry.

Disclosures

The authors have no financial conflicts of interest.

References

1. Rahman, A., and D. A. Isenberg. 2008. Systemic lupus erythematosus. *N. Engl. J. Med.* 358: 929–939.
2. Pathak, S., and C. Mohan. 2011. Cellular and molecular pathogenesis of systemic lupus erythematosus: lessons from animal models. *Arthritis Res. Ther.* 13: 241.
3. Hibbs, M. L., D. M. Tarlinton, J. Armes, D. Grail, G. Hodgson, R. Maglitto, S. A. Stacker, and A. R. Dunn. 1995. Multiple defects in the immune system of Lyn-deficient mice, culminating in autoimmune disease. *Cell* 83: 301–311.
4. Xu, Y., K. W. Harder, N. D. Huntington, M. L. Hibbs, and D. M. Tarlinton. 2005. Lyn tyrosine kinase: accentuating the positive and the negative. *Immunity* 22: 9–18.
5. Scapini, P., S. Pereira, H. Zhang, and C. A. Lowell. 2009. Multiple roles of Lyn kinase in myeloid cell signaling and function. *Immunol. Rev.* 228: 23–40.
6. Smith, K. G., D. M. Tarlinton, G. M. Doody, M. L. Hibbs, and D. T. Fearon. 1998. Inhibition of the B cell by CD22: a requirement for Lyn. *J. Exp. Med.* 187: 807–811.
7. Chan, V. W., C. A. Lowell, and A. L. DeFranco. 1998. Defective negative regulation of antigen receptor signaling in Lyn-deficient B lymphocytes. *Curr. Biol.* 8: 545–553.
8. Scapini, P., Y. Hu, C. L. Chu, T. S. Migone, A. L. Defranco, M. A. Cassatella, and C. A. Lowell. 2010. Myeloid cells, BAFF, and IFN-gamma establish an inflammatory loop that exacerbates autoimmunity in Lyn-deficient mice. *J. Exp. Med.* 207: 1757–1773.
9. Scapini, P., C. Lamagna, Y. Hu, K. Lee, Q. Tang, A. L. DeFranco, and C. A. Lowell. 2011. B cell-derived IL-10 suppresses inflammatory disease in Lyn-deficient mice. *Proc. Natl. Acad. Sci. USA* 108: E823–E832.
10. Krebs, D. L., M. K. Chehal, A. Sio, N. D. Huntington, M. L. Da, P. Ziltener, M. Inglese, N. Kountouri, J. J. Priatel, J. Jones, et al. 2012. Lyn-dependent signaling regulates the innate immune response by controlling dendritic cell activation of NK cells. *J. Immunol.* 188: 5094–5105.
11. Lamagna, C., P. Scapini, J. A. van Ziffle, A. L. DeFranco, and C. A. Lowell. 2013. Hyperactivated MyD88 signaling in dendritic cells, through specific deletion of Lyn kinase, causes severe autoimmunity and inflammation. *Proc. Natl. Acad. Sci. USA* 110: E3311–E3320.
12. Lu, R., G. S. Vidal, J. A. Kelly, A. M. Delgado-Vega, X. K. Howard S. R. Macwana, N. Dominguez, W. Klein, C. Burrell, I. T. Harley, et al; BIOLUPUS and GENLES Multicenter Collaborations. 2009. Genetic associations of LYN with systemic lupus erythematosus. *Genes Immun.* 10: 397–403.
13. Surolia, I., S. P. Pirnie, V. Chellappa, K. N. Taylor, A. Cariappa, J. Moya, H. Liu, D. W. Bell, D. R. Driscoll, S. Diederichs, et al. 2010. Functionally defective germline variants of sialic acid acetylesterase in autoimmunity. *Nature* 466: 243–247.
14. Tsantikos, E., M. J. Maxwell, N. Kountouri, K. W. Harder, D. M. Tarlinton, and M. L. Hibbs. 2012. Genetic interdependence of Lyn and negative regulators of B cell receptor signaling in autoimmune disease development. *J. Immunol.* 189: 1726–1736.
15. Green, N. M., and A. Marshak-Rothstein. 2011. Toll-like receptor driven B cell activation in the induction of systemic autoimmunity. *Semin. Immunol.* 23: 106–112.
16. Nickerson, K. M., S. R. Christensen, J. Shupe, M. Kashgarian, D. Kim, K. Elkon, and M. J. Shlomchik. 2010. TLR9 regulates TLR7- and MyD88-dependent autoantibody production and disease in a murine model of lupus. *J. Immunol.* 184: 1840–1848.
17. Silver, K. L., T. L. Crockford, T. Bouriez-Jones, S. Milling, T. Lambe, and R. J. Cornall. 2007. MyD88-dependent autoimmune disease in Lyn-deficient mice. *Eur. J. Immunol.* 37: 2734–2743.
18. Pisitkun, P., J. A. Deane, M. J. Difilippantonio, T. Tarasenko, A. B. Satterthwaite, and S. Bolland. 2006. Autoreactive B cell responses to RNA-related antigens due to TLR7 gene duplication. *Science* 312: 1669–1672.
19. Subramanian, S., K. Tus, Q.-Z. Li, A. Wang, X.-H. Tian, J. Zhou, C. Liang, G. Bartov, L. D. McDaniel, X. J. Zhou, et al. 2006. A Tlr7 translocation accelerates systemic autoimmunity in murine lupus. *Proc. Natl. Acad. Sci. USA* 103: 9970–9975.
20. Ehlers, M., H. Fukuyama, T. L. McGaha, A. Aderem, and J. V. Ravetch. 2006. TLR9/MyD88 signaling is required for class switching to pathogenic IgG2a and 2b autoantibodies in SLE. *J. Exp. Med.* 203: 553–561.
21. Herlands, R. A., S. R. Christensen, R. A. Sweet, U. Hershberg, and M. J. Shlomchik. 2008. T cell-independent and toll-like receptor-dependent antigen-driven activation of autoreactive B cells. *Immunity* 29: 249–260.
22. Gilliet, M., W. Cao, and Y. J. Liu. 2008. Plasmacytoid dendritic cells: sensing nucleic acids in viral infection and autoimmune diseases. *Nat. Rev. Immunol.* 8: 594–606.
23. Banchereau, J., and V. Pascual. 2006. Type I interferon in systemic lupus erythematosus and other autoimmune diseases. *Immunity* 25: 383–392.
24. Hou, B., P. Saudan, G. Ott, M. L. Wheeler, M. Ji, L. Kuzmich, L. M. Lee, R. L. Coffman, M. F. Bachmann, and A. L. DeFranco. 2011. Selective utilization of Toll-like receptor and MyD88 signaling in B cells for enhancement of the antiviral germinal center response. *Immunity* 34: 375–384.
25. Hou, B., B. Reizis, and A. L. DeFranco. 2008. Toll-like receptors activate innate and adaptive immunity by using dendritic cell-intrinsic and -extrinsic mechanisms. *Immunity* 29: 272–282.
26. Caton, M. L., M. R. Smith-Raska, and B. Reizis. 2007. Notch-RBP-J signaling controls the homeostasis of CD8− dendritic cells in the spleen. *J. Exp. Med.* 204: 1653–1664.
27. Hobeika, E., S. Thiemann, B. Storch, H. Jumaa, P. J. Nielsen, R. Pelanda, and M. Reth. 2006. Testing gene function early in the B cell lineage in mb1-cre mice. *Proc. Natl. Acad. Sci. USA* 103: 13789–13794.
28. Czar, M. J., E. N. Kersh, L. A. Mijares, G. Lanier, J. Lewis, G. Yap, A. Chen, A. Sher, C. S. Duckett, R. Ahmed, and P. L. Schwartzberg. 2001. Altered lymphocyte responses and cytokine production in mice deficient in the X-linked lymphoproliferative disease gene SH2D1A/DSHP/SAP. *Proc. Natl. Acad. Sci. USA* 98: 7449–7454.
29. Itohara, S., P. Mombaerts, J. Lafaille, J. Iacomini, A. Nelson, A. R. Clarke, M. L. Hooper, A. Farr, and S. Tonegawa. 1993. T cell receptor delta gene mutant mice: independent generation of alpha beta T cells and programmed rearrangements of gamma delta TCR genes. *Cell* 72: 337–348.
30. Mombaerts, P., A. R. Clarke, M. L. Hooper, and S. Tonegawa. 1991. Creation of a large genomic deletion at the T-cell antigen receptor beta-subunit locus in mouse embryonic stem cells by gene targeting. *Proc. Natl. Acad. Sci. USA* 88: 3084–3087.
31. Yu, C. C., T. S. Yen, C. A. Lowell, and A. L. DeFranco. 2001. Lupus-like kidney disease in mice deficient in the Src family tyrosine kinases Lyn and Fyn. *Curr. Biol.* 11: 34–38.
32. Radic, M. Z., and M. Weigert. 1994. Genetic and structural evidence for antigen selection of anti-DNA antibodies. *Annu. Rev. Immunol.* 12: 487–520.
33. William, J., C. Euler, S. R. Christensen, and M. J. Shlomchik. 2002. Evolution of autoantibody responses via somatic hypermutation outside of germinal centers. *Science* 297: 2066–2070.
34. Groom, J. R., C. A. Fletcher, S. N. Walters, S. T. Grey, S. V. Watt, M. J. Sweet, M. J. Smyth, C. R. Mackay, and F. Mackay. 2007. BAFF and MyD88 signals promote a lupuslike disease independent of T cells. *J. Exp. Med.* 204: 1959–1971.
35. Crotty, S., E. N. Kersh, J. Cannons, P. L. Schwartzberg, and R. Ahmed. 2003. SAP is required for generating long-term humoral immunity. *Nature* 421: 282–287.
36. Cannons, J. L., S. G. Tangye, and P. L. Schwartzberg. 2011. SLAM family receptors and SAP adaptors in immunity. *Annu. Rev. Immunol.* 29: 665–705.
37. Tsantikos, E., C. Quilici, K. W. Harder, B. Wang, H. J. Zhu, G. P. Anderson, D. M. Tarlinton, and M. L. Hibbs. 2009. Perturbation of the CD4 T cell compartment and expansion of regulatory T cells in autoimmune-prone Lyn-deficient mice. *J. Immunol.* 183: 2484–2494.
38. Gutierrez, T., J. M. Mayeux, S. B. Ortega, N. J. Karandikar, Q. Z. Li, D. Rakheja, X. J. Zhou, and A. B. Satterthwaite. 2013. IL-21 promotes the production of anti-DNA IgG but is dispensable for kidney damage in $lyn^{-/-}$ mice. *Eur. J. Immunol.* 43: 382–393.
39. Coffman, R. L., A. Sher, and R. A. Seder. 2010. Vaccine adjuvants: putting innate immunity to work. *Immunity* 33: 492–503.
40. Tsantikos, E., S. A. Oracki, C. Quilici, G. P. Anderson, D. M. Tarlinton, and M. L. Hibbs. 2010. Autoimmune disease in Lyn-deficient mice is dependent on an inflammatory environment established by IL-6. *J. Immunol.* 184: 1348–1360.
41. Gross, A. J., I. Proekt, and A. L. DeFranco. 2011. Elevated BCR signaling and decreased survival of Lyn-deficient transitional and follicular B cells. *Eur. J. Immunol.* 41: 3645–3655.
42. Shahaf, G., A. J. Gross, M. Sternberg-Simon, D. Kaplan, A. L. DeFranco, and R. Mehr. 2012. Lyn deficiency affects B-cell maturation as well as survival. *Eur. J. Immunol.* 42: 511–521.
43. Meade, J., C. Fernandez, and M. Turner. 2002. The tyrosine kinase Lyn is required for B cell development beyond the T1 stage in the spleen: rescue by overexpression of Bcl-2. *Eur. J. Immunol.* 32: 1029–1034.
44. Merrell, K. T., R. J. Benschop, S. B. Gauld, K. Aviszus, D. Decote-Ricardo, L. J. Wysocki, and J. C. Cambier. 2006. Identification of anergic B cells within a wild-type repertoire. *Immunity* 25: 953–962.
45. Hwang, S. H., H. Lee, M. Yamamoto, L. A. Jones, J. Dayalan, R. Hopkins, X. J. Zhou, F. Yarovinsky, J. E. Connolly, M. A. Curotto de Lafaille, et al. 2012. B cell TLR7 expression drives anti-RNA autoantibody production and exacerbates disease in systemic lupus erythematosus-prone mice. *J. Immunol.* 189: 5786–5796.
46. Walsh, E. R., P. Pisitkun, E. Voynova, J. A. Deane, B. L. Scott, R. R. Caspi, and S. Bolland. 2012. Dual signaling by innate and adaptive immune receptors is required for TLR7-induced B-cell-mediated autoimmunity. *Proc. Natl. Acad. Sci. USA* 109: 16276–16281.
47. Rawlings, D. J., M. A. Schwartz, S. W. Jackson, and A. Meyer-Bahlburg. 2012. Integration of B cell responses through Toll-like receptors and antigen receptors. *Nat. Rev. Immunol.* 12: 282–294.
48. Oracki, S. A., E. Tsantikos, C. Quilici, A. Light, T. Schmidt, A. M. Lew, J. E. Martin, K. G. Smith, M. L. Hibbs, and D. M. Tarlinton. 2010. CTLA4Ig alters the course of autoimmune disease development in $Lyn^{-/-}$ mice. *J. Immunol.* 184: 757–763.
49. Wofsy, D. 1993. Treatment of murine lupus with anti-CD4 monoclonal antibodies. *Immunol. Ser.* 59: 221–236.
50. Shlomchik, M. J. 2009. Activating systemic autoimmunity: B's, T's, and tolls. *Curr. Opin. Immunol.* 21: 626–633.
51. Cline, A. M., and M. Z. Radic. 2004. Murine lupus autoantibodies identify distinct subsets of apoptotic bodies. *Autoimmunity* 37: 85–93.
52. Pao, L. I., K. P. Lam, J. M. Henderson, J. L. Kutok, M. Alimzhanov, L. Nitschke, M. L. Thomas, B. G. Neel, and K. Rajewsky. 2007. B cell-specific deletion of protein-tyrosine phosphatase Shp1 promotes B-1a cell development and causes systemic autoimmunity. *Immunity* 27: 35–48.

53. Jellusova, J., U. Wellmann, K. Amann, T. H. Winkler, and L. Nitschke. 2010. CD22 x Siglec-G double-deficient mice have massively increased B1 cell numbers and develop systemic autoimmunity. *J. Immunol.* 184: 3618–3627.
54. Hermiston, M. L., A. L. Tan, V. A. Gupta, R. Majeti, and A. Weiss. 2005. The juxtamembrane wedge negatively regulates CD45 function in B cells. *Immunity* 23: 635–647.
55. Zikherman, J., R. Parameswaran, M. Hermiston, and A. Weiss. 2013. The structural wedge domain of the receptor-like tyrosine phosphatase CD45 enforces B cell tolerance by regulating substrate specificity. *J. Immunol.* 190: 2527–2535.
56. Gross, A. J., J. R. Lyandres, A. K. Panigrahi, E. T. Prak, and A. L. DeFranco. 2009. Developmental acquisition of the Lyn-CD22-SHP-1 inhibitory pathway promotes B cell tolerance. *J. Immunol.* 182: 5382–5392.